

Site characterization of the INGV station IV.CDCA - Città di Castello

Working Group: Giuseppe DI GIULIO Maurizio VASSALLO Paola BORDONI Giovanna CULTRERA Daniela FAMIANI Giuliano MILANA Luciana CANTORE	Date: June 2016
Subject: Final report illustrating measurements, analysis and results at IV.CDCA station	

1	
1. Introduction.....	3
2	
2. Geophysical investigation.....	4
2.1 Array Measurements Results	5
3	
3. Vs Model.....	11
4	
4. Conclusions.....	14
Disclaimer and limits of use of information.....	15
Esclusione di responsabilità e limiti di uso delle informazioni.....	16

1. Introduction

In this report, we present the geophysical measurements and the results obtained in the framework of the 2016 agreement between INGV and DPC, named “*Allegato B2: Obiettivo 1 (Responsabile: C. Meletti) - TASK B: Caratterizzazione siti accelerometrici (Responsabili: P. Bordoni, F. Pacor)*” for the characterization of sites of the Italian National Seismic Network (RSN) with accelerometers.

Here the results for station IV-CDCA are presented.

Geophysical measurements are two 2D arrays of seismic stations in passive configuration. Using surface-wave analysis, we provide results in terms of dispersion curves that are inverted to obtain shear-wave velocity (V_s) profiles for the studied area. The inverted models are suitable for computing the average V_s velocity in the uppermost 30 m (V_{s30}) and assigning then the EC8 soil class category.



2. Geophysical investigation

IV.CDCA station is situated in the park (“Parco Ansa del Tevere”) of Città di Castello (Perugia, Italy).

Figure 1 shows the location of the seismic stations used for the two 2D arrays deployed in the target area surrounding IV.CDCA.



Figure 1: Plan view of the two 2D seismic arrays deployed around IV-CMPO site. The yellow and cyan points indicate the fourteen stations of the 2D array in passive configuration (named “small” and “big” array, respectively). All stations are equipped with Reftek R130 digitizer and Lennartz 3D-5sec velocimetric sensors. IV-CDCA station is situated in proximity of the sa00 station.

2.1 ARRAY MEASUREMENTS RESULTS

Two 2D arrays were performed using 14 single seismic stations equipped with Reftek 130 digitizers and Lennartz 3d-5s velocimetric sensors. Figure 1 shows their position, and hereinafter we referred to these two arrays as “*big*” and “*small*” array. The common noise recording lasted approximately 2 hours for both arrays. The measurements were recorded the 15th of June 2016. The *small* and *big* array are characterized by a maximum aperture of 145 and 260 m, respectively. A view of field work is shown in Figure 2. The seismic sensors were positioned in a two-dimensional geometry with irregular spacing, as shown in Figure 2 (some stations of the two arrays shared the same position).

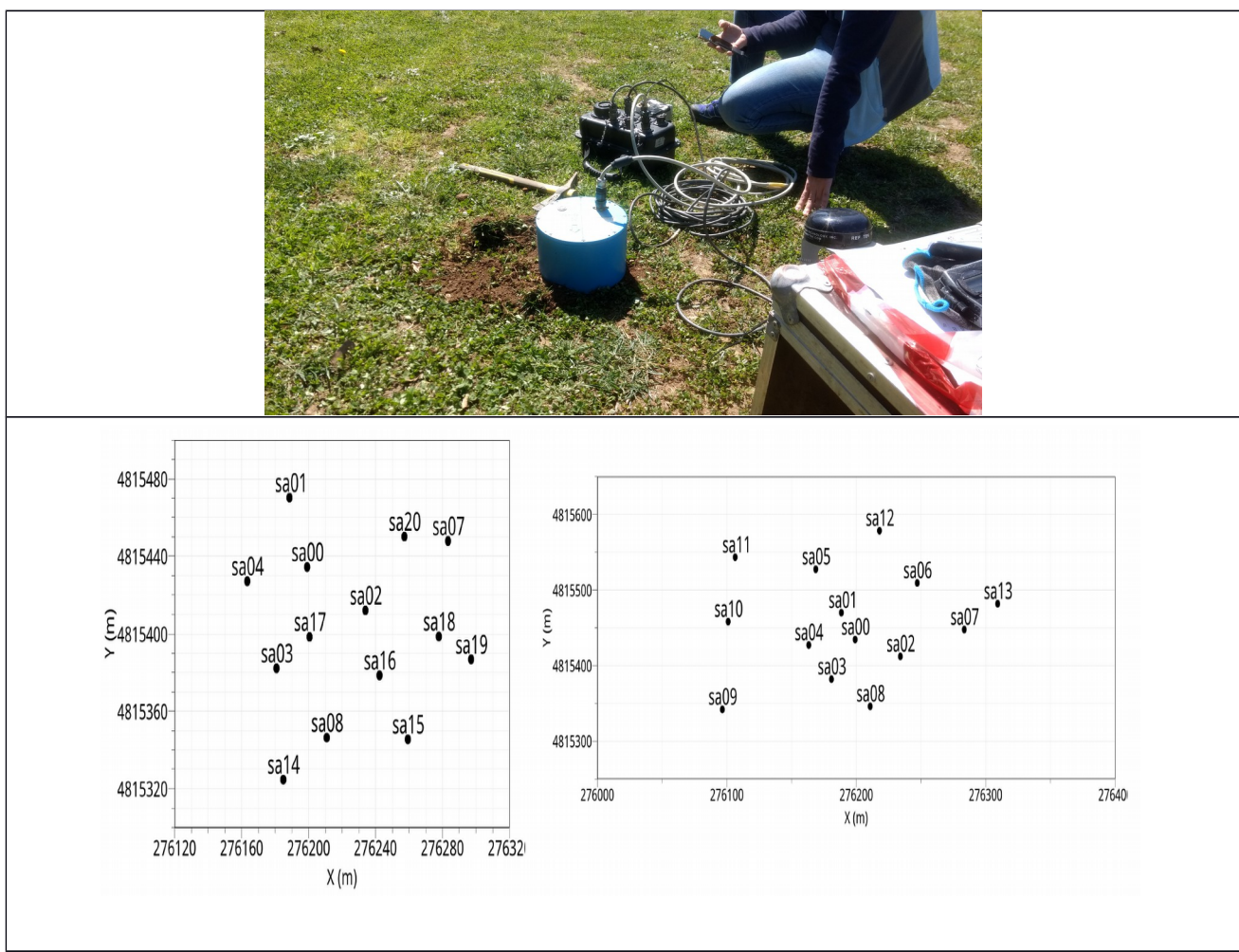


Figure 2: Top: Example of an installation of a seismic station. **Bottom:** 2D Array geometry of the *small* (left panel) and *big* (right panel) array.

The geometries of the arrays allow the performance in terms of wavenumbers described in Figure 3, where the theoretical Array Transfer Function is reported for each array.

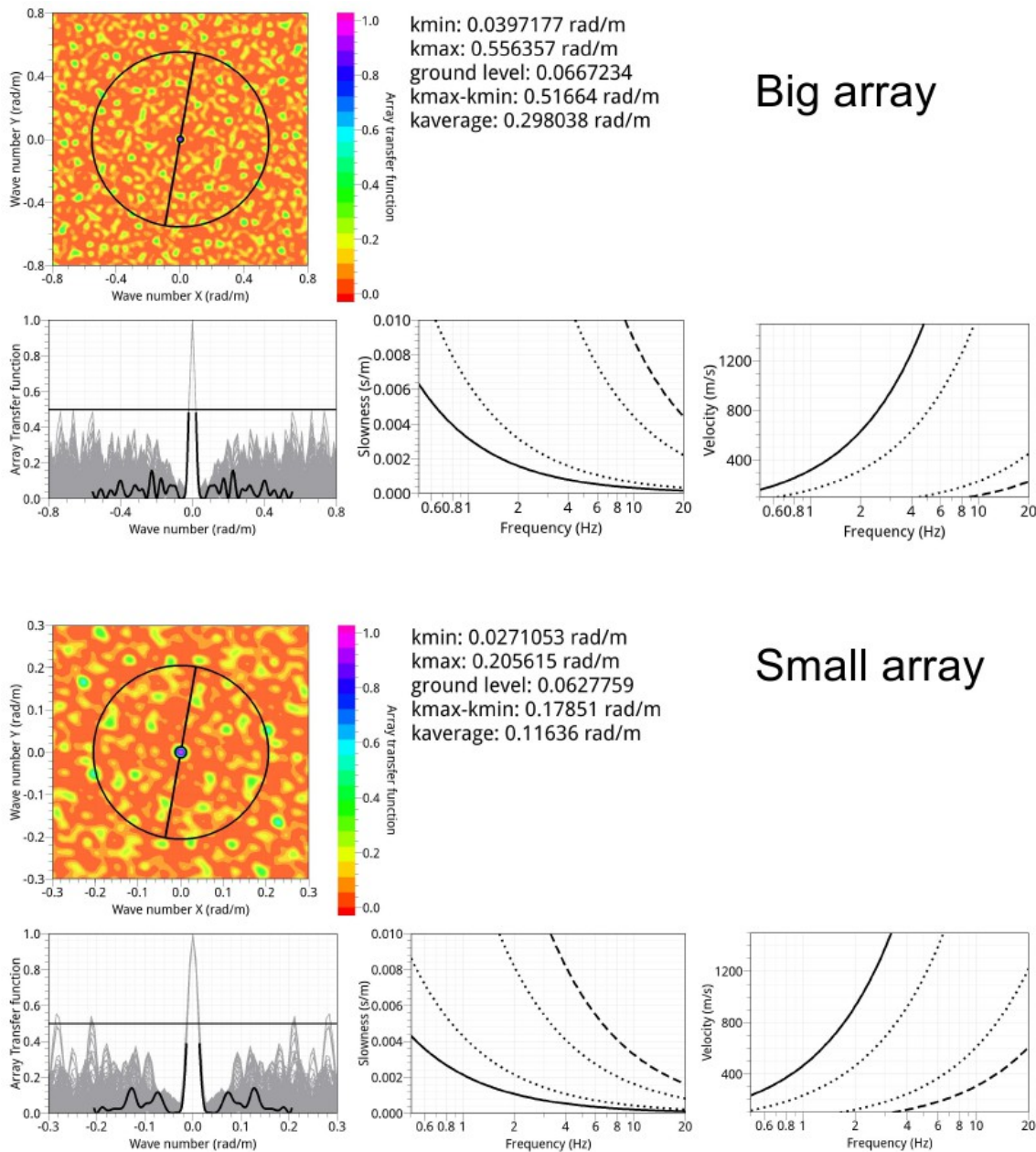


Figure 3: Theoretical Array Transfer function of the two 2D arrays installed in the target area of IV-CDCA. Alias and resolution curves are also reported in the slowness(or velocity)-frequency representation.

The computed H/V curves of the 14 stations are overimposed for each array in Figure 4. There is a general agreement of the H/V shapes in almost the entire reliable frequency band (eigenfrequency of the velocimetric sensor is 0.2 Hz). The resonance frequency (F_0) can be assigned to 0.42 Hz, even if the H/V curves show an amplified band up to 0.6 Hz. The rotated HV spectral ratios show consistently amplification in this frequency band (see Figure 5 where we show for semplicity only the results of the *big* array).

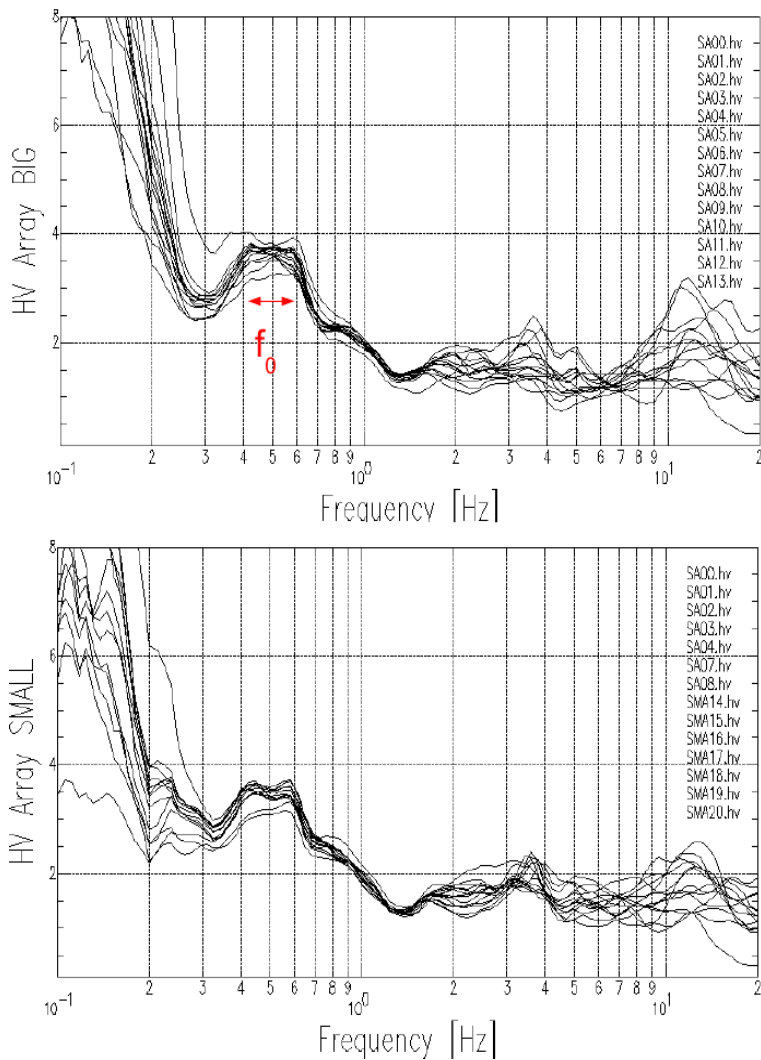


Figure 4: H/V curves of the 14 stations for the *big* (top panel) and *small* array (bottom panel).

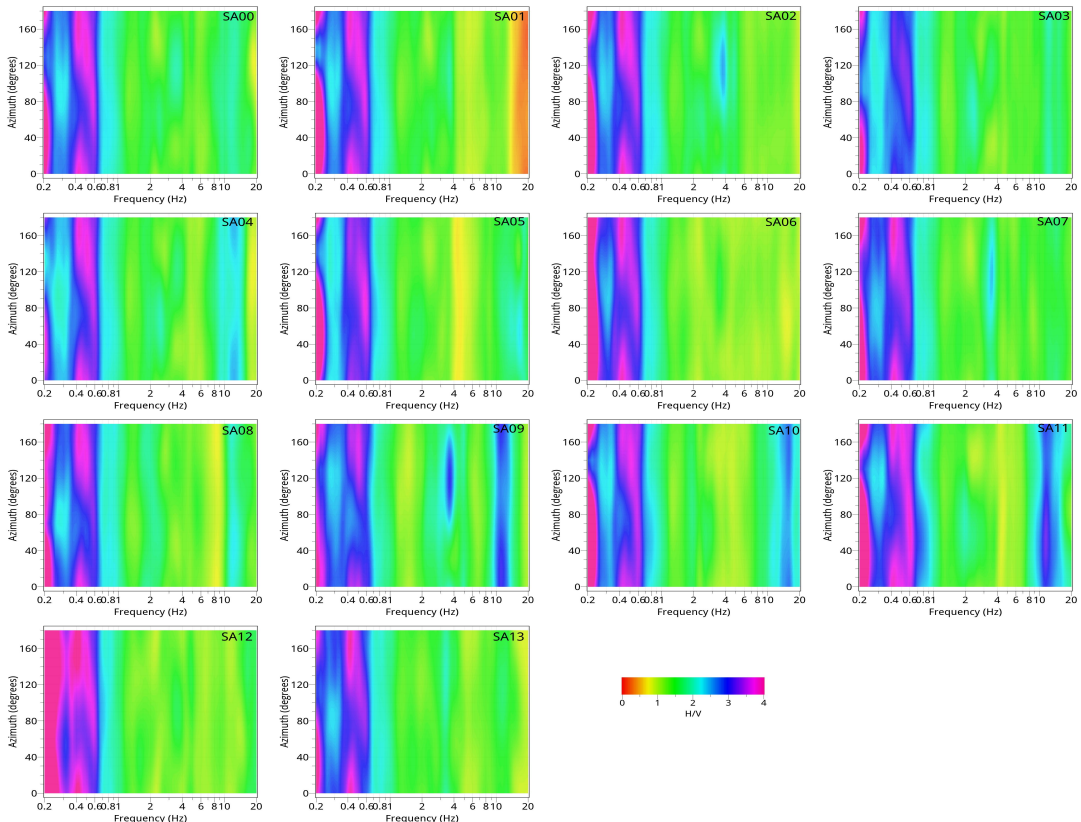


Figure 5: Rotating H/V curves at the 14 stations of the *big* array..

Data from the 2D arrays have been analysed in terms of conventional frequency-wavenumber (FK) analysis and high-resolution FK analysis. Because the two techniques lead to similar results, we present hereinafter only the results of the conventional FK method.

The FK analysis was performed on the three-components of motion; the results using the horizontal and vertical components were interpreted in terms of Rayleigh and Love surface waves, respectively. We used the GEOPSY code (<http://www.geopsy.org>) for the H/V computation and surface-wave analysis. Figure 6a shows the dispersion curves derived from the f-k analysis using the vertical signal recorded by the *big* and *small* array. Because the picked dispersion curves of the two arrays show a slight discrepancy in terms of apparent values (about 50 m/s; see Figure 6b), we decided to average them.

The surface-wave analysis performed on the horizontal signal provides the dispersion curves shown in Figure 7. Also in this case, the two curves were averaged to obtain a mean dispersion curve.

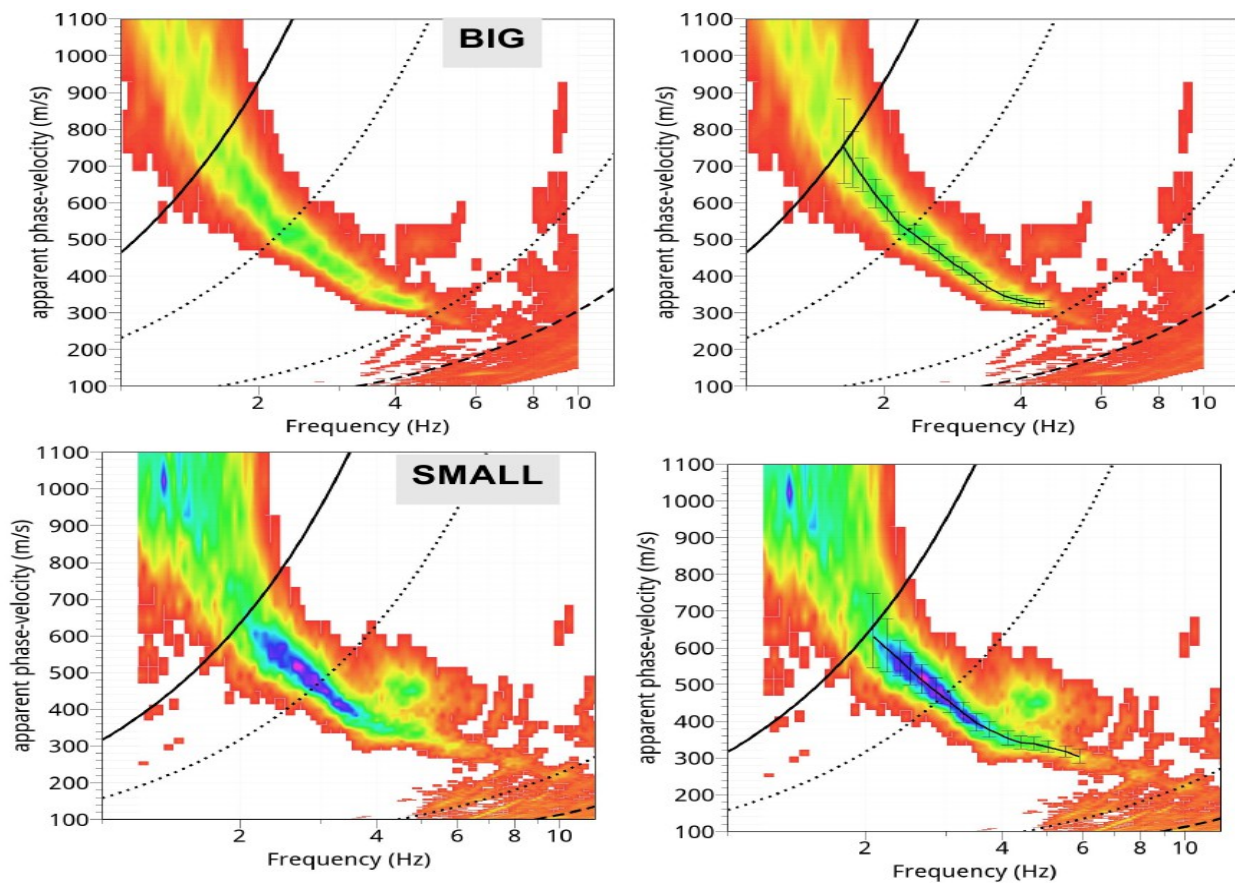


Figure 6a: Unpicked and picked dispersion curve in the velocity-frequency plan for the big (top) and small array (bottom panel) working with the vertical component.

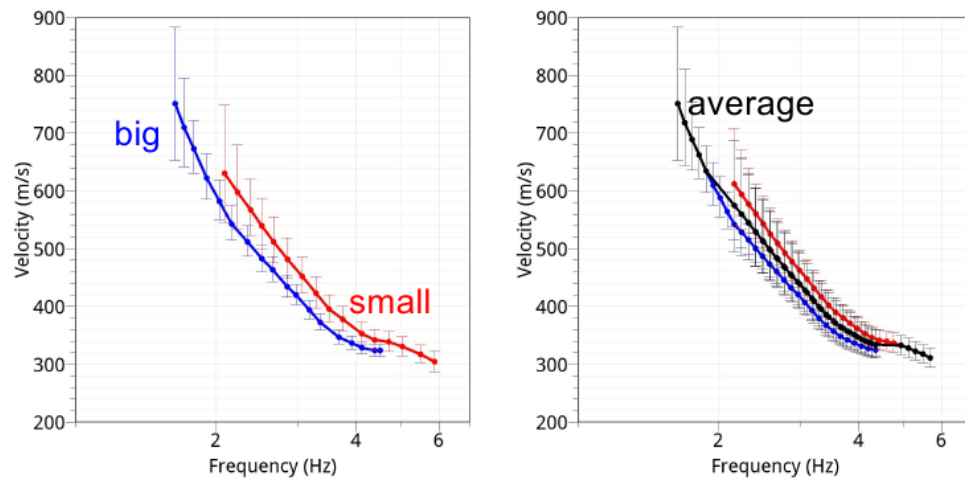


Figure 6b: Left) The picked dispersion curve from the big and small array are overimposed (blue and red curve, respectively). The vertical bars indicate uncertainties. Right) To proceed with the inversion step, we averaged the two dispersion curves: the black mean curve was considered during the inversion step.

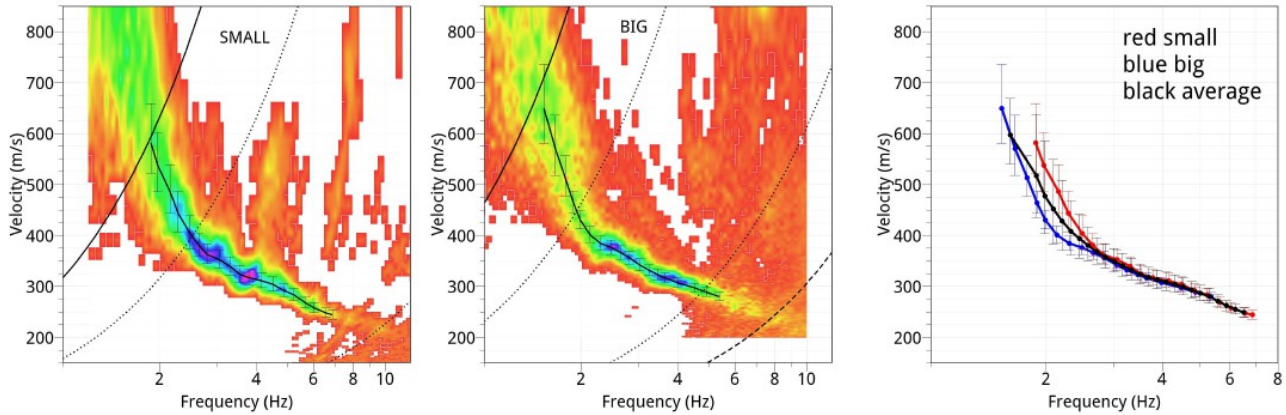


Figure 7: Picked dispersion curve for the small (left) and big array (middle panel) working with the horizontal component. The dispersion curves derived from these two arrays were compared in the right panel, where the black curve indicates the average curve.

The final dispersion curves selected for the inversion step are shown in Figure 8 assuming Rayleigh and Love fundamental mode (for vertical and horizontal components, respectively). The selected part of H/V curve to be considered in the ellipticity inversion is also shown.

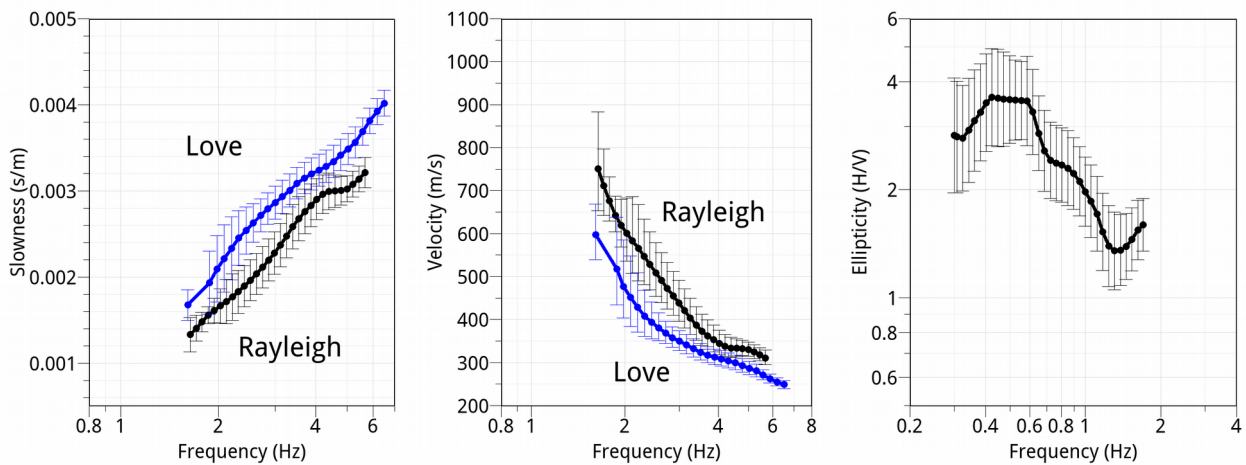


Figure 8: Dispersion and H/V curves considered during the inversion process. Rayleigh (black) and Love (blue) dispersions were derived from the analysis on vertical and horizontal component, respectively.

3. Vs Model

To proceed with the inversion step, we assume that the dispersion curves derived from the vertical and horizontal component of motion are associated to the fundamental mode of Rayleigh and Love waves, respectively.

To summarize, the targets during our inversion process were:

- 1) Dispersion curves as shown in Figure 8.
- 2) Ellipticity curve in terms of Rayleigh fundamental mode extracted from the most similar part of the H/V curves (from 0.3 to 1.8 Hz; see the right panel of Figure 8)
- 3) Fundamental frequency ($F_0=0.42$ Hz)

The resulting models obtained after a preliminary inversion are shown in Figure 9. We used a simple model parameterization composed of two main layers over halfspace, where in the first layer a shear-wave velocity increasing with depth was allowed (following a power-law, see the zoomed view of Figure 9).

Focusing on the Vs models, the Vs is increasing from 110-150 to 600-700 m/s for the first layer (180 m thick); the Vs is of about 1000 m/s for the second layer (approximately from 180 to 650 m deep). The halfspace is found by the inversion at about 600-700 m deep.

However we noted some discrepancy between theoretical and field curve (Figure 9); this could indicate a too simple model space parameterization or some assumptions in the interpretation of the field curves not fully matched.

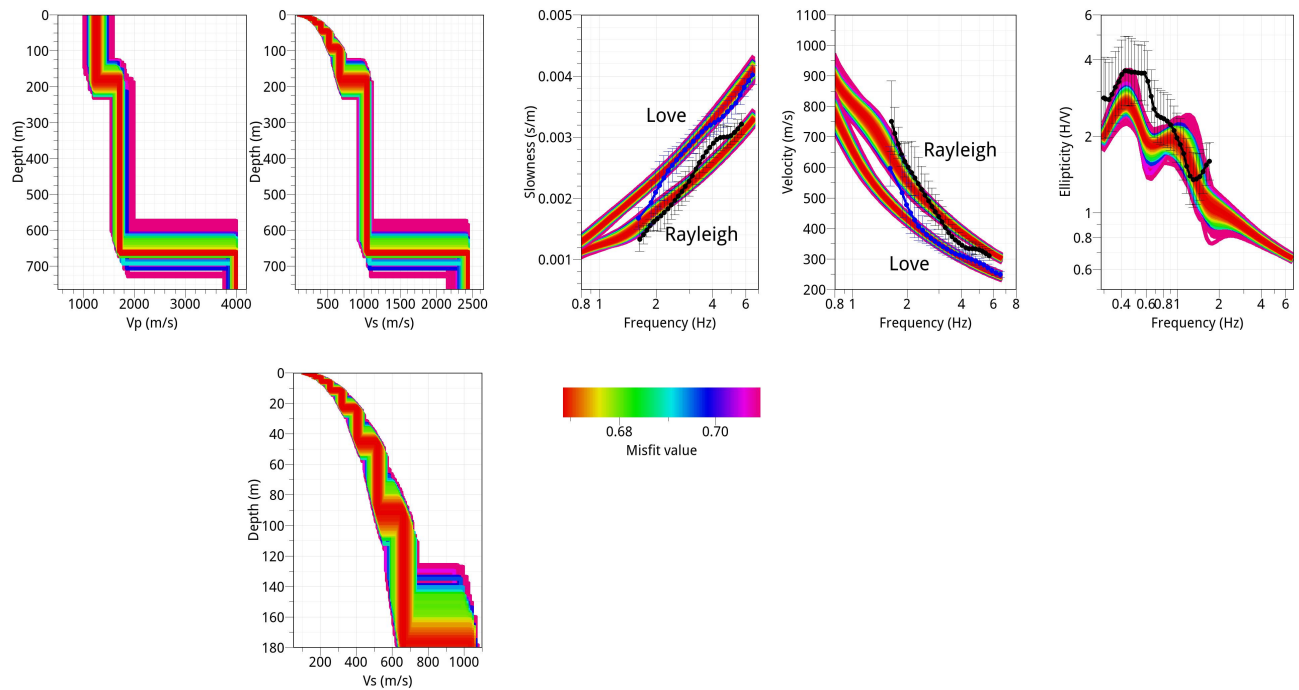


Figure 9: Resulting models after the inversion of the dispersion and H/V ellipticity curves (the field data are shown as black curves). A zoom of the Vs profile is shown in the bottom.

The best V_p and V_s model (i.e. lowest misfit) resulting from the inversion are proposed in Figure 10 and Table 1.

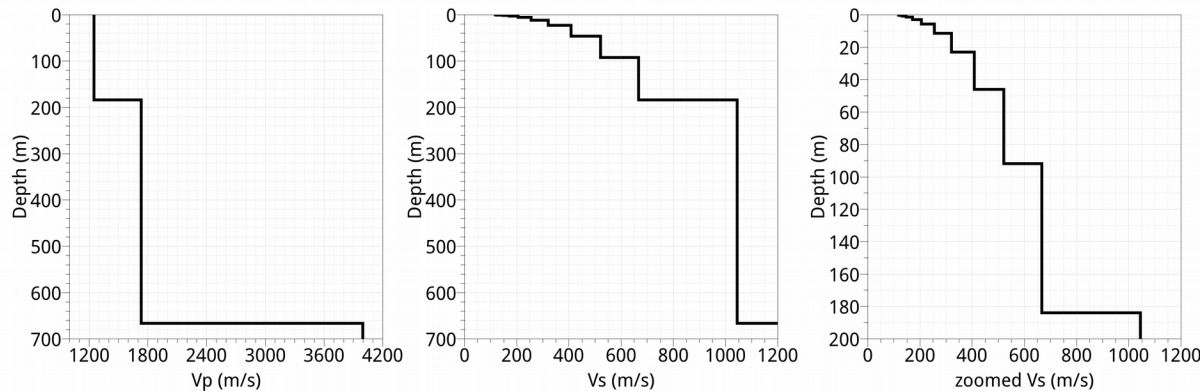


Figura 10: Best-fit model of V_p and V_s profiles [extracted from the ensemble of Fig. 9]. A zoomed view of V_s profile is shown on the right.

From (m)	To (m)	Thickness (m)	V_s (m/s)	V_p (m/s)
0	0,1	0,1	115	1248
0,1	0,17	0,07	118	1248
0,17	0,36	0,19	123	1248
0,36	0,7	0,34	132	1248
0,7	1,4	0,7	147	1248
1,4	2,9	1,5	171	1248
2,9	5,7	2,8	206	1248
5,7	11,4	5,7	255	1248
11,4	22,9	11,5	321	1248
22,9	45,9	23	408	1248
45,9	92	46,1	521	1248
92	184	92	667	1248
184	666	482	1044	1733
666	?	?	2433	4000

Table 1: Best-fit model

4. Conclusions

The surface-wave analysis at IV.CDCA station indicates a soft site. Because the H/V curves show amplification from 0.42 to 0.6 Hz, a first resonant peak is found doubtfully at 0.42 Hz. However these low-frequency resonant values (< 1 Hz) suggest a bedrock relatively deep. The preliminary inversion shows Vs models with a significant seismic contrast at a depth of about 150-200 m, where the Vs increases from 650 to 1100 m/s (Figures 9, 10 and Table 1). The uppermost layer shows low Vs value (< 350 m/s up to 23 m deep; see Table 1). The V_{s30} retrieved from the best inverted model is 275 m/s (Table 2), therefore IV-CMPO is classified as soil class C following the NTC08 seismic classification.

V_{s30} (m/s)	Soil class
275	C

Table 2: Soil Class

Disclaimer and limits of use of information

The INGV, in accordance with the Article 2 of Decree Law 381/1999, carries out seismic and volcanic monitoring of the Italian national territory, providing for the organization of integrated national seismic network and the coordination of local and regional seismic networks as described in the agreement with the Department of Civil Protection.

INGV contributes, within the limits of its skills, to the evaluation of seismic and volcanic hazard in the Country, according to the mode agreed in the ten-year program between INGV and DPC February 2, 2012 (Prot. INGV 2052 of 27/2/2012), and to the activities planned as part of the National Civil Protection System.

In particular, this document¹ has informative purposes concerning the observations and the data collected from the monitoring and observational networks managed by INGV.

INGV provides scientific information using the best scientific knowledge available at the time of the drafting of the documents produced; However, due to the complexity of natural phenomena in question, nothing can be blamed to INGV about the possible incompleteness and uncertainty of the reported data.

INGV is not responsible for any use, even partial, of the contents of this document by third parties and any damage caused to third parties resulting from its use.

The data contained in this document is the property of the INGV.



This document is licensed under License

Attribution – No derivatives 4.0 International (CC BY-ND 4.0)

¹This document is level 3 as defined in the "Principi della politica dei dati dell'INGV (D.P. n. 200 del 26.04.2016)"

Esclusione di responsabilità e limiti di uso delle informazioni

L'INGV, in ottemperanza a quanto disposto dall'Art.2 del D.L. 381/1999, svolge funzioni di sorveglianza sismica e vulcanica del territorio nazionale, provvedendo all'organizzazione della rete sismica nazionale integrata e al coordinamento delle reti sismiche regionali e locali in regime di convenzione con il Dipartimento della Protezione Civile.

L'INGV concorre, nei limiti delle proprie competenze inerenti la valutazione della Pericolosità sismica e vulcanica nel territorio nazionale e secondo le modalità concordate dall'Accordo di programma decennale stipulato tra lo stesso INGV e il DPC in data 2 febbraio 2012 (Prot. INGV 2052 del 27/2/2012), alle attività previste nell'ambito del Sistema Nazionale di Protezione Civile.

In particolare, questo documento¹ ha finalità informative circa le osservazioni e i dati acquisiti dalle Reti di monitoraggio e osservative gestite dall'INGV.

L'INGV fornisce informazioni scientifiche utilizzando le migliori conoscenze scientifiche disponibili al momento della stesura dei documenti prodotti; tuttavia, in conseguenza della complessità dei fenomeni naturali in oggetto, nulla può essere imputato all'INGV circa l'eventuale incompletezza ed incertezza dei dati riportati.

L'INGV non è responsabile dell'utilizzo, anche parziale, dei contenuti di questo documento da parte di terzi e di eventuali danni arrecati a terzi derivanti dal suo utilizzo.

La proprietà dei dati contenuti in questo documento è dell'INGV.



Quest'opera è distribuita con Licenza

Creative Commons Attribuzione - Non opere derivate 4.0 Internazionale.

¹Questo documento rientra nella categoria di livello 3 come definita nei "Principi della politica dei dati dell'INGV (D.P. n. 200 del 26.04.2016)".